A first-principles investigation of electronic, magnetic and optical properties of CeP for optoelectronic applications

Student ID: 171331
Session: 2017-2018

Report submitted to the Department of Physics at
Jashore University of Science and Technology
in partial fulfillment of the requirements
for the degree of Bachelor of Science
with Honours in Physics

December 2022

Abstract

The electronic, magnetic, and optical properties of cerium phosphide (CeP) are studied in this work by using the full-potential linearized augmented plane wave (FP-LAPW) approach in the framework of the density functional theory (DFT). The generalized gradient approximation proposed by Perdew, Burke, and Ernzerhof (GGA-PBE) and Tran-Blaha modified Becke-Johnson (TB-mBJ) approaches are used to approximate the exchange correlation potential. Both zinc-blende (ZB) and rock salt (RS) type structures of CeP are used to calculate the ferromagnetic (FM) and non-magnetic (NM) phases. The results show that, the calculations of the total energy are clearly favor the ground state and the equilibrium lattice constants are in good agreement with exprimental values. For the FM phase of the ZB type structure, the electronic band structure and density of state (DOS) calculations reveal a band gap, represent CeP has semiconducting behavior. The total magnetic moment of this type structure follows the Slater-Pauling rule. Ability of CeP for optoelectronic device manufacturing is demonstrated by estimated optical parameters such as dielectric function, refractive index, reflectivity, absorption coefficient, and conductivity.

Acknowledgements

I praise and thank almighty Allah, the Lord of the worlds, the Most Merciful, the Guider of hearts, the Provider of sustenance, the Owner of life and death.

I want to express my cordial gratitude to my supervisor Dr.Mohammad Abdur Rashid, for his enthusiasm, patience, helpful information and earnest support, that have helped me tremendously at all times in my research and writing of this project.

I really appreciate all of the faculty members of Department of Physics for their invaluable advice and assistance. I want to express my gratitude to all of my groupmates who either directly or indirectly assisted me to finish my project report.

I also want to express my sincere gratitude to my parents for always supporting me both morally and financially.

Contents

List of Figures

List of Tables

A first-principles investigation of electronic, magnetic and optical properties of CeP for optoelectronic applications

Chapter 1

Introduction

Semiconductors are essential in modern technology and provides us a comfortable existence on this planet. Because of their excellent electronic, magnetic and optical properties, they exhibit many fascinating applications with light-emitting and laser diodes, transistors, IC's, circuit fabrication, solar cells, organic Nano-Radio Frequency Identification Devices, Metal Insulator Semiconductor Photo-detectors, Electro-Optic Waveguide Modulators, and heterostructure lasers [1, 2]. Early research on rare earth elements reveal their semiconducting and other intriguing characteristics. Our investigated compound CeP also shows semiconducting behavior with indirect bandgap, where Ce is classified as a rare-earth element in the periodic table. Since rare-earth elements are an important part of many high-tech products, this calculation with CeP provides an excellent electronic, magnetic, and optical properties [3]. Our calculation is done for FM and NM phases of both ZB and RS type structures, and we find that the FM phase of the ZB type structure has more interesting electronic and optical properties [4, 5]. The band structure calculation, of this ferromagnetic ZB type structure gives an indirect bandgap between the conduction and the valence band, which represent the semiconducting feature of it. Semiconducting behavior of CeP must be fascinating because they play such a crucial part in modern electronics. The study of CeP brings us closer to future

calculations for more fascinating systems, potentially opening a new era in modern electronics. The goal of this report is to calculate the electronic, magnetic, and optical properties of CeP compound using first-principles calculations based on density functional theory (DFT) and the full potential linearized augmented plane waves (FP-LAPW) [6] method as implemented in the WIEK2k code [7], which is a Fortran computer program for solving the Kohn-Sham equations of DFT. Because of their widespread use in spintronic applications, rare-earth elements become an essential members of the periodic table. Spintronics are the study of the intrinsic spin of electrons and the magnetic moment associated with it. Our CeP-based calculation exhibits a variety of intriguing characteristics, such as semiconducting behavior for its ferromagnetic ordering. By observing this calculation we can make more interesting future investigation, which expand the spintronic fields. This research is divided into four sections: 1. Introduction, 2. Density Functional Theory, 3. Electronic, magnetic and optical properties of CeP, and 4. Conclusion. In chapter 1 we highlight the most important and promising uses of our compound CeP. We discuss basic quantum mechanics and density functional theory in chapter 2, and our calculations are based on this theory. We explained and interpreted the findings of our calculations in chapter 3. In this chapter we also discuss why CeP is a fascinating ingredient. In chapter 4 we examined that CeP is a potential candidate as a future applicant.

Chapter 2

Density Functional Theory

2.1 Schrödinger equation

Erwin Schrödinger's attempt to describe the so-called 'matter wave' in 1926, which is named after him. The time-dependent single particle Schrödinger equation,

$$i\hbar\frac{\partial}{\partial t}\Psi(\vec{r},t) = \hat{H}\Psi(\vec{r},t) \tag{2.1}$$

It is a linear and homogeneous equation for the wave function Ψ [8]. Where the Hamiltonian

$$\hat{H} = \hat{T} + \hat{V} = -\frac{\hbar^2}{2m}\vec{\nabla}^2 + V(\vec{r},t) \tag{2.2}$$

Which gives the time-dependent Schrödinger equation for a particle moving in a potential

$$i\hbar\frac{\partial}{\partial t}\Psi(\vec{r},t) = [-\frac{\hbar^2}{2m}\vec{\nabla}^2 + V(\vec{r},t)]\Psi(\vec{r},t) \tag{2.3}$$

For N particles in three dimensions the Hamiltonian is,

$$\hat{H} = \sum_i^N \frac{\hat{p_i^2}}{2m_i} + V(\vec{r}_1,\vec{r}_2,...,\vec{r}_N,t) = -\frac{\hbar^2}{2}\sum_{i=1}^N \frac{1}{m_i} + V(\vec{r}_1,\vec{r}_2,...,\vec{r}_N,t) \tag{2.4}$$

The corresponding Schrödinger equation reads

$$i\hbar\frac{\partial}{\partial t}\Psi(\vec{r}_1,\vec{r}_2,...,\vec{r}_N,t)=[-\frac{\hbar^2}{2}\sum_{i=1}^{N}\frac{1}{m_i}\vec{\nabla}^2+V(\vec{r}_1,\vec{r}_2,...,\vec{r}_N,t)]\Psi(\vec{r}_1,\vec{r}_2,...,\vec{r}_N,t) \tag{2.5}$$

This is the time-dependent Schrödinger equation for many-body system. When the Hamiltonian itself has no time-dependency then we get the time-independent Schrödinger equation. In this case the potential does not depend on time, like as $V(\vec{r}_1,\vec{r}_2,...,\vec{r}_N,t)$. So the Hamiltonian

$$\hat{H}=-\frac{\hbar^2}{2m}\vec{\nabla}^2+V(\vec{r}) \tag{2.6}$$

The time-independent equation is obtained by the approach of separation of variables. The spatial and temporal part of the wave function can be separated by this way,

$$\Psi(\vec{r}_1,\vec{r}_2,...,\vec{r}_N,t)=\Psi(\vec{r}_1,\vec{r}_2,...,\vec{r}_N)\tau(t)=\Psi(\vec{r}_1,\vec{r}_2,...,\vec{r}_N).e^{-i\omega t} \tag{2.7}$$

So, the time-independent Schrödinger equation for many-body system can be written as

$$E\Psi(\vec{r}_1,\vec{r}_2,...,\vec{r}_N)=[-\frac{\hbar^2}{2}\sum_{i=1}^{N}\frac{1}{m_i}\nabla_i^2+V(\vec{r}_1,\vec{r}_2,...,\vec{r}_N)]\Psi(\vec{r}_1,\vec{r}_2,...,\vec{r}_N) \tag{2.8}$$

The general eigenvalue equation becomes as

$$E\Psi(\vec{r}_1,\vec{r}_2,...,\vec{r}_N)=\hat{H}\Psi(\vec{r}_1,\vec{r}_2,...,\vec{r}_N) \tag{2.9}$$

2.2 The wave function

In the previous section we can see the detail about Schrödinger equation, where the term wave function was repeatedly used. The Schrödinger equation determines how wave functions evolve over time. In this section we can see about the wave function. The first and most important postulate is that the state of a particle is completely described by it's (time-dependent) wave function, i.e. the wave function contains all

information about the particle's state [9]. The wave function itself has no physical interpretation. The square of the absolute value of the wave function has a physical interpretation and known as a probability density

$$|\Psi(\vec{r}_1, \vec{r}_2, ..., \vec{r}_N)|^2 d\vec{r}_1, d\vec{r}_2, ..., d\vec{r}_N. \tag{2.10}$$

Equation (2.10) describes the probability that particles $1, 2, ..., N$ are located simultaneously in the corresponding volume element $d\vec{r}_1, d\vec{r}_2, ..., d\vec{r}_N$ [10]. If the positions of two particles are exchanged the overall probability density cannot depend on such an exchange, i.e.

$$|\Psi(\vec{r}_1, \vec{r}_2, ..., \vec{r}_i, \vec{r}_j, ..., \vec{r}_N)|^2 = |\Psi(\vec{r}_1, \vec{r}_2, ..., \vec{r}_i, \vec{r}_j, ..., \vec{r}_N)|^2 \tag{2.11}$$

The integral of the probability density overall the system's degrees of freedom must be 1 in accordance with the probability interpretation. This general requirement that a wave function must satisfy is called the normalization condition. Which is,

$$\int d\vec{r}_1 \int d\vec{r}_2 ... \int d\vec{r}_N |\Psi(\vec{r}_1, \vec{r}_2, ..., \vec{r}_N)|^2 = 1 \tag{2.12}$$

This condition is also required for a physical acceptable wave function. The wave function must be continuous over the full spatial range and square-integratable [11]. We can calculate expectation values of operators with a wave function provides the expectation value of the corresponding observable for that wave function [12]. For an observable $O(\vec{r}_1, \vec{r}_2, ..., \vec{r}_N)$ written as,

$$O = \langle O \rangle = \int d\vec{r}_1 \int d\vec{r}_2 ... \int d\vec{r}_N \Psi^*(\vec{r}_1, \vec{r}_2, ..., \vec{r}_N) \hat{O} \Psi(\vec{r}_1, \vec{r}_2, ..., \vec{r}_N) \tag{2.13}$$

2.3 Born-Oppenheimer (BO) approximation

The Hamiltonian of a many-body system consisting of nuclei and electrons can be written as:

$$H_{tot} = -\sum_I \frac{\hbar^2}{2M_I}\nabla^2_{\vec{R}_I} - \sum_i \frac{\hbar^2}{2m_e}\nabla^2_{\vec{r}_i} + \frac{1}{2}\sum_{\substack{I,J \\ I\neq J}} \frac{Z_I Z_J e^2}{|\vec{R}_I - \vec{R}_J|} + \frac{1}{2}\sum_{\substack{i,j \\ i\neq j}} \frac{e^2}{|\vec{r}_i - \vec{r}_j|} - \sum_{I,i} \frac{Z_I e^2}{|\vec{R}_I - \vec{r}_i|} \tag{2.14}$$

Where the indexes I,J run on nuclei, i and j on electrons, $\vec{R}_I$ and M_I are positions and masses of the nuclei, $\vec{r}_i$ and m_e of the electrons, Z_I the atomic number of nucleus I. The first term is the kinetic energy of the nuclei, the second term is the kinetic energy of the electrons, the third term is the potential energy of nucleus - nucleus Coulomb interaction, the fourth term is the potential energy of electron-electron Coulomb interaction and the last term is the potential energy of nucleus-electron Coulomb interaction. The time-independent Schrödinger equation for the system

$$H_{tot}\Psi(\{\vec{R}_I\},\{\vec{r}_i\}) = E\Psi(\{\vec{R}_I\},\{\vec{r}_i\}) \tag{2.15}$$

Where $\Psi(\{\vec{R}_I\},\{\vec{r}_i\})$ is the total wave function of the system. By solving the above Schrödinger equation we get wave function, which can provide everything about the system. It is quietly impossible to solve it in practice and approximation is needed. A so-called Born-Oppenheimer approximation was made by Born and Oppenheimer [13] in 1927. Since the nuclei are much heavier than electrons, the nuclei move much slower than the electrons. Therefore we can separate the movement of nuclei and electrons. So, the electronic wave function depends upon only the nuclear position but does not depend upon their velocities. The total wave function can be written as

$$\Psi(\{\vec{R}_I\},\{\vec{r}_i\}) = \Theta(\{\vec{R}_I\})\phi(\{\vec{r}_i\};\{\vec{R}_I\}) \tag{2.16}$$

Where $\Theta(\{\vec{R}_I\})$describe the nuclei and $\phi(\{\vec{r}_i\};\{\vec{R}_I\})$ the electrons. So, we can write the Schrödinger equation into two separate equation

$$H_e\phi(\{\vec{r}_i\};\{\vec{R}_I\}) = V(\{\vec{R}_I\})\phi(\{\vec{r}_i\};\{\vec{R}_I\}) \tag{2.17}$$

Where

$$H_e = -\sum_i \frac{\hbar^2}{2m_e}\nabla^2_{\vec{r}_i} + \frac{1}{2}\sum_{\substack{I,J \\ I\neq J}} \frac{Z_I Z_J e^2}{|\vec{R}_I - \vec{R}_J|} + \frac{1}{2}\sum_{\substack{i,j \\ i\neq j}} \frac{e^2}{|\vec{r}_i - \vec{r}_j|} - \sum_{I,i} \frac{Z_I e^2}{|\vec{R}_I - \vec{r}_i|} \tag{2.18}$$

and

$$[-\sum_I \frac{\hbar^2}{2M_I}\nabla^2_{\vec{R}_I} + V(\{\vec{R}_I\})]\Theta(\{\vec{R}_I\}) = E'\Theta(\{\vec{R}_i\}) \tag{2.19}$$

Equation (2.17) is the equation for the electronic problem with the nuclei positions fixed. The significance of the BO approximation is to separate the movement of electrons and nuclei.

2.4 The Hartree-Fock approach

The Hartree-Fock method seeks to approximately solve the electronic Schrödinger equation, and it assumes that the wave function can be approximated by a single slater determinant made up of one spin orbital per electron. Hence, for now only the electronic Schrödinger equation is of interest, therefore in the following sections we set $\hat{H} \equiv \hat{H}_{el}$, $E \equiv E_{el}$, and so on. The energy as observable corresponding to the Hamilton operator, therefore the energy can be calculated as

$$E = \langle \hat{H} \rangle = \int d\vec{r}_1 \int d\vec{r}_2 ... \int d\vec{r}_N \Psi^*(\vec{r}_1, \vec{r}_2, ..., \vec{r}_N)\hat{H}\Psi(\vec{r}_1, \vec{r}_2, ..., \vec{r}_N) \tag{2.20}$$

The central idea of the Hartree-Fock approach is that the energy obtained by any trial wave function and

$$E_{trial} \geq E_0 \tag{2.21}$$

Where, E_0 is the lowest or ground state energy of the system.

$$E_{trial} = \int d\vec{r}_1 \int d\vec{r}_2 ... \int d\vec{r}_N \Psi^*_{trial}(\vec{r}_1, \vec{r}_2, ..., \vec{r}_N)\hat{H}\Psi_{trial}(\vec{r}_1, \vec{r}_2, ..., \vec{r}_N) \tag{2.22}$$

and

$$E_0 = \int d\vec{r}_1 \int d\vec{r}_2 ... \int d\vec{r}_N \Psi^*_0(\vec{r}_1, \vec{r}_2, ..., \vec{r}_N)\hat{H}\Psi_0(\vec{r}_1, \vec{r}_2, ..., \vec{r}_N) \tag{2.23}$$

In accordance to bra-ket notation [14] equation (2.21) to (2.23) can be written as

$$\langle \Psi_{trial} | \hat{H} | \Psi_{trial} \rangle = E_{trial} \geq E_0 = \langle \Psi_0 | \hat{H} | \Psi_0 \rangle \tag{2.24}$$

Proof: The trial wave function Φ_{trial} can be expressed as linear combination of the eigenfunctions Ψ_i ,

$$\Psi_{trial} = \sum_i \lambda_i \Psi_i \tag{2.25}$$

This trial wave function is normalized so

$$\langle \Psi_{trial} | \Psi_{trial} \rangle = 1 = \langle \sum_i \lambda_i \Psi_i | \sum_j \lambda_j \Psi_j \rangle = \sum_i \sum_j \lambda_i^* \lambda_j \langle \Psi_i | \Psi_j \rangle = \sum_j |\lambda_j|^2. \tag{2.26}$$

From equation (2.24) and (2.26) we get

$$E_{trial} = \langle \Psi_{trial} | \hat{H} | \Psi_{trial} \rangle = \langle \sum_i \lambda_i \Psi_i | \hat{H} | \sum_j \lambda_j \Psi_j \rangle = \sum_j E_j |\lambda_j|^2. \tag{2.27}$$

Also,

$$E_{trial} = \sum_j E_j |\lambda_j|^2 \geq E_0 \sum_j |\lambda_j|^2. \tag{2.28}$$

The mathematical framework used above, i.e. rules which assign numerical values to functions, so called functional, is also one of the main concept in density functional theory. A function gets a numerical input and generates a numerical output whereas a functional gets a function as input and generates a numerical output [15]. Equations (2.20) to (2.28) also include that a search for the minimal energy value while applied on all allowed N-electron wave functions will always provide the ground-state wave function. Expressed in terms of functional calculus, where $\Psi \to N$ addresses all allowed N-electron wave functions, that is

$$E_0 = \min_{\Psi \to N} E[\Psi] = \min_{\Psi \to N} \langle \Psi | \hat{H} | \Psi \rangle = \min_{\Psi \to N} \langle \Psi | \hat{T} + \hat{V} + \hat{U} | \Psi \rangle. \tag{2.29}$$

In the Hartree-Fock approach, the search is restricted to approximations of the N-electron wave function by an antisymmetric product of N one-electron wave functions, the so called spin-orbitals $X_i(\vec{x}_i)$. A wave function of this type is called

slater-determinant, and reads

$$\Psi_0 \approx \phi_{SD} = (N!)^{-\frac{1}{2}} \begin{vmatrix} X_1(\vec{x}_1) & X_2(\vec{x}_1) & \cdots & X_N(\vec{x}_1) \\ X_1(\vec{x}_2) & X_2(\vec{x}_2) & \cdots & X_N(\vec{x}_2) \\ \vdots & \vdots & \ddots & \vdots \\ X_1(\vec{x}_N) & X_2(\vec{x}_N) & \cdots & X_N(\vec{x}_N) \end{vmatrix} \tag{2.30}$$

Returning to the variational principle and equation (2.29), the ground state energy approximated by a single slater determinant becomes

$$E_0 = \min_{\phi_{SD}\to N} E[\phi_{SD}] = \min_{\phi_{SD}\to N} \langle\phi_{SD}|\hat{H}|\phi_{SD}\rangle = \min_{\phi_{SD}\to N} \langle\phi_{SD}|\hat{T}+\hat{V}+\hat{U}|\phi_{SD}\rangle \tag{2.31}$$

A general expression for the Hartree-Fock energy is obtained by usage of the Slater determinant as a trial function

$$E_{HF} = \langle\phi_{SD}|\hat{H}|\phi_{SD}\rangle = \langle\phi_{SD}|\hat{T}+\hat{V}+\hat{U}|\phi_{SD}\rangle \tag{2.32}$$

The final expression for the Hartree-Fock energy contains three major parts:

$$E_{HF} = \langle\phi_{SD}|\hat{H}|\phi_{SD}\rangle = \sum_i^N (i|\hat{h}|i) + \frac{1}{2}\sum_i^N\sum_j^N [(ii|jj) - (ij|ji)] \tag{2.33}$$

With

$$(i|\hat{h_i}|i) = \int X_i^*(\vec{x}_i)[-\frac{1}{2}\vec{\nabla}_i^2 - \sum_{k=1}^M \frac{Z_k}{r_{ik}}]X_i(\vec{x}_i)d\vec{x}_i, \tag{2.34}$$

$$(ii|jj) = \iint |X_i(\vec{x}_i)|^2 \frac{1}{r_{ij}} |X_j(\vec{x}_j)|^2 d\vec{x}_i d\vec{x}_j, \tag{2.35}$$

$$(ii|jj) = \iint X_i(\vec{x}_i)X_j^*(\vec{x}_j)\frac{1}{r_{ij}}X_j(\vec{x}_j)X_i^*(\vec{x}_i)d\vec{x}_i d\vec{x}_j. \tag{2.36}$$

The first term corresponds to the kinetic energy and the nucleus-electron interactions, $\hat{h}$ denoting the single particle contribution of the Hamiltonian, whereas the latter two terms correspond to electron-electron interactions. They are called Coulomb and exchange integral, respectively. Examination of equations (2.33) to (2.36) furthermore reveals, that the Hartree-Fock energy can be expressed as a functional of the spin orbitals $E_{HF} = E[X_i]$. Thus, variation of the spin orbitals leads to

the minimum energy. The spin orbitals remain orthonormal during minimization, so we get

$$\hat{f}X_i = \lambda_i X_i \qquad i = 1, 2, ..., N \tag{2.37}$$

With

$$\hat{f}_i = -\frac{1}{2}\vec{\nabla}_i^2 - \sum_{k=1}^{M}\frac{Z_k}{r_{ik}} + \sum_{i}^{N}[\hat{J}_j(\vec{x}_i) - \hat{K}_j(\vec{x}_i)] = \hat{h}_i + \hat{V}^{HF}(i), \tag{2.38}$$

the Fock operator for the i-th electron. Where, the first two terms represent the kinetic and potential energy due to nucleus-electron interaction, collected in the core Hamiltonian $\hat{h}_i$, whereas the latter terms are sums over the Coulomb operators $\hat{J}_j$ and the exchange operators $\hat{K}_j$ with the other j electrons, which form the Hartree-Fock potential $\hat{V}^{HF}$. There the major approximation of Hartree-Fock can be seen. The two electron repulsion operator from the original Hamiltonian is exchange by a one-electron operator $\hat{V}^{HF}$. which describes the repulsion in average.

2.4.1 Limitations and failings of the Hartree-Fock approach

Since a many electron wave function cannot be described entirely by a single Slater determinant, the energy obtained by HF calculations is always larger than the exact ground state energy. The most accurate energy obtainable by HF-methods is called the Hartree-Fock-limit. The difference between E_{HF} and E_{exact} is called correlation energy and can be denoted as [16]

$$E_{corr}^{HF} = E_{min} - E_{HF} \tag{2.39}$$

2.5 The electron density

In an electronic system, the number of electrons per unit volume in a given state is the electron density for that state. For a system of N electrons with wave function Ψ the electron density is defined as

$$n(\vec{r}) = N\sum_{s_1}\int d\vec{x}_2 ... \int d\vec{x}_N \Psi^*(\vec{x}_1, \vec{x}_2, ..., \vec{x}_N)\Psi(\vec{x}_1, \vec{x}_2, ..., \vec{x}_N). \tag{2.40}$$

Which is the basic variable of density functional theory. If the spin coordinates are neglected, the electron density can even be expressed as measurable observable only dependent on spatial coordinates

$$n(\vec{r}) = N \int d\vec{r}_2 ... \int d\vec{r}_N \Psi^*(\vec{r}_1, \vec{r}_2, ..., \vec{r}_N)\Psi(\vec{r}_1, \vec{r}_2, ..., \vec{r}_N). \tag{2.41}$$

The total number of electron can be obtained by integration the electron density over the spatial variables

$$N = \int d\vec{r} n(\vec{r}). \tag{2.42}$$

2.6 Thomas-Fermi model

The predecessor to DFT was the Thomas-Fermi model named after Llewellyn Thomas and Enrico Fermi [17] in 1927. In this method, they uesd the electron density $n(\vec{r})$ as the basic variable instead of the wave function. The total energy of a system in an external potential $V_{ext}(\vec{r})$ is written as a functional of the electron density $n(\vec{r})$ as:

$$E_{TF}[n(\vec{r})] = A_1 \int n(\vec{r})^{\frac{5}{3}} d\vec{r} + \int n(\vec{r}) V_{ext}(\vec{r}) d\vec{r} + \frac{1}{2} \iint \frac{n(\vec{r}) n(\vec{r}')}{|\vec{r} - \vec{r}'|} d\vec{r} d\vec{r}' \tag{2.43}$$

Where the first term is the kinetic energy of the non-interacting electrons in a homogeneous electron gas (HEG) with $A_1 = \frac{3}{10}(3\pi^2)^{\frac{2}{3}}$ in atomic units. The kinetic energy density of a HEG is obtained by adding up all of the free-electron energy state $\varepsilon_k = \frac{k^2}{2}$ up to the Fermi wave vector $k_F = [3\pi^2 n(\vec{r})]^{\frac{1}{3}}$ as:

$$t_0[n(\vec{r})] = \frac{2}{(2\pi)^3} \int_0^{k_F} \frac{k^2}{2} 4\pi k^2 dk = A_1 n(\vec{r})^{\frac{5}{3}} \tag{2.44}$$

The second term is the classical electrostatic energy of the nucleus-electron Coulomb interaction. The third term is the classical electrostatic Hartree energy approximated by the classical Coulomb repulsion between electrons. In 1930, Dirac extended the Thomas-Fermi method by adding a local exchange term $A_2 \int n(\vec{r})^{\frac{4}{3}} d\vec{r}$ to

equation (2.43) with $A_2 = -\frac{3}{4}(\frac{3}{\pi})^{\frac{1}{3}}$, which leads equation (2.43) to

$$E_{TFD}[n(\vec{r})] = A_1 \int n(\vec{r})^{\frac{5}{3}} d\vec{r} + \int n(\vec{r}) V_{ext}(\vec{r}) d\vec{r} + \frac{1}{2} \iint \frac{n(\vec{r}) n(\vec{r}')}{|\vec{r} - \vec{r}'|} d\vec{r} d\vec{r}' + A_2 \int n(\vec{r})^{\frac{4}{3}} d\vec{r} \tag{2.45}$$

The solution can be found as

$$\delta\{E_{TFD}[n(\vec{r})] - \mu(\int n(\vec{r}) - N)\} = 0 \tag{2.46}$$

Where μ is the chemical potential. Equation (2.46) leads to the Thomas-Fermi-Dirac equation

$$\frac{5}{3} A_1 \int n(\vec{r})^{\frac{2}{3}} + V_{ext}(\vec{r}) + \int \frac{n(\vec{r}')}{|\vec{r} - \vec{r}'|} d\vec{r}' + \frac{4}{3} A_2 n(\vec{r})^{\frac{1}{3}} - \mu = 0 \tag{2.47}$$

Which can be solved directly to obtain the ground state density. The most serious one is that the theory fails to describe bonding between atoms, thus molecules and solids cannot form in this theory [18]. Although it is not good enough to describe electrons in matter, its concept to use electron density as the basic variable illustrate the way DFT works.

2.7 The Hohenberg-Khon theorems

The heart of DFT is the Hohenberg-Kohn (HK) theorem. This theorem is invented by Hohenberg and Kohn in 1964. This theorem tells us that not only $n(\vec{r})$ is a functional of $v(\vec{r})$ but that also $v(\vec{r})$ is up to a constant determined by $n(\vec{r})$ uniquely. The electronic Hamiltonian operator be written as $\hat{H}_e l = \hat{T} + \hat{V} + \hat{U}$, Where $\hat{V}$ represent the external potential. The energy of the system can be denoted as

$$E = \langle \Psi | \hat{H} | \Psi \rangle = \langle \Psi | \hat{T} + \hat{V} + \hat{U} | \Psi \rangle = \int v(\vec{r}) n(\vec{r}) d\vec{r} + \langle \Psi | \hat{T} + \hat{U} | \Psi \rangle \tag{2.48}$$

Which will be used for the proof of Hohenberg and Kohn's first theorem.

2.7.1 Theorem 1

The external potential $v(\vec{r})$ is a functional of the electron density $n(\vec{r})$ and, up to an unimportant constant, uniquely determined by it.

Proof: For simplicity, here only consider the case that the ground state of the system is nondegenerate. It is assumed that there exist two external potentials $v(\vec{r})$ and $v'(\vec{r})$ which differ by more than just a trivial constant also both potentials give rise to the same electron density $n(\vec{r})$. The Hamiltonian $\hat{H}$ and $\hat{H}'$, the wave function Ψ and Ψ' are different from each other also the energies E and E' associated with the particular wave function different. Then the expression,

$$E_0' = \langle\Psi'|\hat{H}'|\Psi'\rangle < \langle\Psi|\hat{H}'|\Psi\rangle = \langle\Psi|\hat{H}+\hat{V}'-\hat{V}|\Psi\rangle = \langle\Psi|\hat{H}|\Psi\rangle+\langle\Psi|\hat{V}'-\hat{V}|\Psi\rangle \quad (2.49)$$

and

$$E_0 = \langle\Psi|\hat{H}|\Psi\rangle < \langle\Psi'|\hat{H}'|\Psi'\rangle = \langle\Psi'|\hat{H}'+\hat{V}-\hat{V}'|\Psi'\rangle = \langle\Psi'|\hat{H}'|\Psi'\rangle + \langle\Psi'|\hat{V}-\hat{V}'|\Psi'\rangle \quad (2.50)$$

are obtained. By the use of (2.48), this can be rewritten as

$$E_0 < E_0 + \int [v'(\vec{r}) - v(\vec{r})]n(\vec{r})d\vec{r} \quad (2.51)$$

and

$$E_0 < E_0' + \int [v(\vec{r}) - v'(\vec{r})]n(\vec{r})d\vec{r} \quad (2.52)$$

By summation of (2.51) and (2.52) the inequality

$$E_0' + E_0 < E_0 + E_0' \quad (2.53)$$

is obtained, which represents an inconsistency and therefore provides by *reductioadabsurdum* the proof that $v(\vec{r})$ is truly a unique functional of $n(\vec{r})$.

2.7.2 Theorem 2

The ground state energy can be derived from the electron density by the use of variational calculus. The electron density, which provides a minimum of the ground state energy, is therefore the exact ground state density. Since the wave function is a unique functional of the electron density, every trial wave function Ψ' corresponds to a trial density $n'(\vec{r})$ following equation(2.41). According to the Rayleigh-Ritz principle, the ground state energy is obtained as

$$E_{v,0} = \min_{\Psi'} \langle \Psi' | \hat{H} | \Psi' \rangle \tag{2.54}$$

Proof: In principle, the minimization can be carried out in two steps. In the first step, a trial electron density $n'(\vec{r})$ is fixed. The class of trial functions corresponding to that electron density is then denoted by $\Psi'^{\alpha}_{n'}$. Then, the constrained energy minimum is defined as

$$[E_v[n'(\vec{r})]] \equiv \min_{\alpha} \langle \Psi'^{\alpha}_{n'} | \hat{H} | \Psi'^{\alpha}_{n'} \rangle = \int v(\vec{r}) n'(\vec{r}) d\vec{r} + F[n'(\vec{r})]. \tag{2.55}$$

In that notation, $F[n'(\vec{r})]$ is the universal functional

$$F[n'(\vec{r})] \equiv \min_{\alpha} \langle \Psi'^{\alpha}_{n'} | \hat{T} + \hat{U} | \Psi'^{\alpha}_{n'} \rangle \tag{2.56}$$

Equation (2.55) is minimized over all trial densities $n'(\vec{r})$:

$$E_{v,0} = \min_{n'(\vec{r})} E_v[n'(\vec{r})] = \min_{n'(\vec{r})} \{ \int v(\vec{r}) n'(\vec{r}) d\vec{r} + F[n'(\vec{r})] \} \tag{2.57}$$

Now, for a non-degenerate ground state, the energy in 2.57 is attained, if $n'(\vec{r})$ is the actual ground state density. It has been shown that density functional theory provides a clear and mathematical exact framework for the use of the electron density as base variable. Nevertheless, nothing of what has been derived is of practical use. In other words, the Hohenberg-Kohn theorems, as important as they are, do not provide any help for the calculation of molecular properties and also do not provide any information about approximations for functional like $F[n'(\vec{r})]$. This difficulties

was overcome by Kohn and Sham in 1965, who proposed the well known Kohn-Sham equations.

2.8 The Kohn-Sham (KS) equations

The KS method was so successful that Khon was honored the Nobel prize in chemistry in 1998. This method puts Hohenberg-Kohn theorems into practical use and makes DFT calculations possible with even a single personal computer. The most desirable way in which quantities can be calculated for problems without an exact analytical solution is one that allows iterations. An early example of an iterative approach are the self-consistent single particle Hartree equations. Hartree's approximation assumes that every electron moves in an effective single-particle potential of the form

$$v_H(\vec{r}) = -\frac{Z}{|\vec{r}|} + \int \frac{n(\vec{r}')}{|\vec{r} - \vec{r}'|} d\vec{r}'. \tag{2.58}$$

The first term is an attractive Coulomb potential of a nucleus with atomic number Z, whereas the integral term corresponds to the potential caused by the mean electron density distribution $n(\vec{r})$. The mean density can be denoted in terms of the single particle wave functions

$$n(\vec{r}) = \sum_{j=1}^{M} |\phi_j(\vec{r})|^2. \tag{2.59}$$

It is important to mention that the sum in (2.59) runs over the M lowest eigenvalues in accordance to the Pauli principle. The 3N-dimensional Schrödinger equation for electrons moving in an effective potential written as

$$[-\frac{1}{2}\vec{\nabla}^2 + v_H(\vec{r})]\phi_j(\vec{r}) = \epsilon_j \phi_j(\vec{r}) \qquad j = 1, ..., N \tag{2.60}$$

Therefore, Khon and Sham investigated the density functional theory applied to a system of N non-interacting electrons in an external potential, similar to Hartree's approach. Recalling (2.55) and (2.56), the expression for the energy of such a system is of the form

$$E_{v(\vec{r})}[n'(\vec{r})] \equiv \int v(\vec{r}) n'(\vec{r}) d\vec{r} + T_S[n'[(\vec{r})] \geq E \tag{2.61}$$

Where $n'(\vec{r})$ is a v-representable density for non-interacting electrons and $T_S[n'[(\vec{r})]$ the kinetic energy of the ground state of those non-interacting electrons [19]. Set up of the Euler-Lagrange equation for the non-interacting case (2.61) with the density defined in (2.59) as argument provides

$$\delta E_v[n'(\vec{r})] \equiv \int \delta n'(\vec{r})[v(\vec{r}) + \frac{\delta}{\delta n'(\vec{r})} T_S[n'[(\vec{r})]|_{n'(\vec{r})=n(\vec{r})} - \epsilon] d\vec{r} = 0 \tag{2.62}$$

With $n'(\vec{r})$, the exact ground state density for the potential $v(\vec{r})$, and the Lagrangian multiplier ϵ to ensure particle density conservation. For a system of non-interacting electrons, the total ground state energy and particle density can therefore simply be denoted as the sums

$$E = \sum_{(j=1)}^{N} \epsilon_j \tag{2.63}$$

and

$$n(\vec{r}) = \sum_{(j=1)}^{N} |\phi_j(\vec{r})|^2. \tag{2.64}$$

In addition, Kohn and Sham used the universal functional in equations (2.55) to (2.57) as an alternative formulation, namely

$$F[n'(\vec{r})] \equiv T_S[n'(\vec{r})] + \frac{1}{2} \int \frac{[n'(\vec{r})][n'(\vec{r}')]}{|\vec{r} - \vec{r}'|} d\vec{r} d\vec{r}' + E_{xc}[n'(\vec{r})] \tag{2.65}$$

In (2.65) $T_S[n'(\vec{r})]$ is the kinetic energy functional of non-interacting electrons and the second term is the so-called Hartee term which describes the electrostatic self-repulsion of the electron density. The last term is called exchange-correlation term. It is implicitly defined by (2.65) and can in practice only be approximated. The quality of the approximation for $E_{xc}[n'(\vec{r})]$ is therefore one of the key issues in DFT. Construction of the Euler-Lagrange equations for the interacting case in equation (2.65) provides

$$\delta E_v[n'(\vec{r})] \equiv \int \delta n'(\vec{r})[v_{eff}(\vec{r}) + \frac{\delta}{\delta n'(\vec{r})} T_S[n'[(\vec{r})]|_{n'(\vec{r})=n(\vec{r})} - \epsilon] d\vec{r} = 0 \tag{2.66}$$

with

$$v_{eff}(\vec{r}) \equiv v(\vec{r}) + \int \frac{[n(\vec{r}')]}{|\vec{r} - \vec{r}'|} d\vec{r}' + v_{xc}(\vec{r}) \tag{2.67}$$

and the functional derivative

$$v_{xc}(\vec{r}) \equiv \frac{\delta}{\delta n'(\vec{r})} E_{xc}[n'(\vec{r})]|_{n'(\vec{r})=n(\vec{r})} \tag{2.68}$$

Whereas the Euler-Lagrange equation resembles (2.68) up to the potential term. Because of that, the minimizing density can be calculated in a way similar to the Hartree-approach described in equations (2.58) to (2.60). The corresponding equations are the single-particle Schrödinger equation

$$[-\frac{1}{2}\vec{\nabla}^2 + v_{eff}(\vec{r})]\phi_j(\vec{r}) = \epsilon_j \phi_j(\vec{r}) \qquad j = 1, ..., N \tag{2.69}$$

as well as the defining equation for the particle density

$$n(\vec{r}) = \sum_{j=1}^{M} |\phi_j(\vec{r})|^2, \tag{2.70}$$

Which form together with the effective potential v_{eff} in (2.67) the self-consistent Kohn-Sham equations. The accurate ground state energy, as one of the most important quantities, can be expressed as

$$E = \sum_j \epsilon_j + E_{xc}[n(\vec{r})] - \int v_{xc}(\vec{r}) n(\vec{r}) dv - \frac{1}{2} \int \frac{[n(\vec{r}')][n(\vec{r}')]}{|\vec{r} - \vec{r}'|} d\vec{r} d\vec{r}' \tag{2.71}$$

Equation (2.71) can be seen as an generalization of the energy expression obtained with the Hartree-approach. Similar to the Hohenberg-Kohn theorems, also equations (2.69) to (2.71) are formally exact, which means, if exact $E_{xc}[n(\vec{r})]$ and $v_{xc}[n(\vec{r})]$ would be used, one would obtain the exact solution.

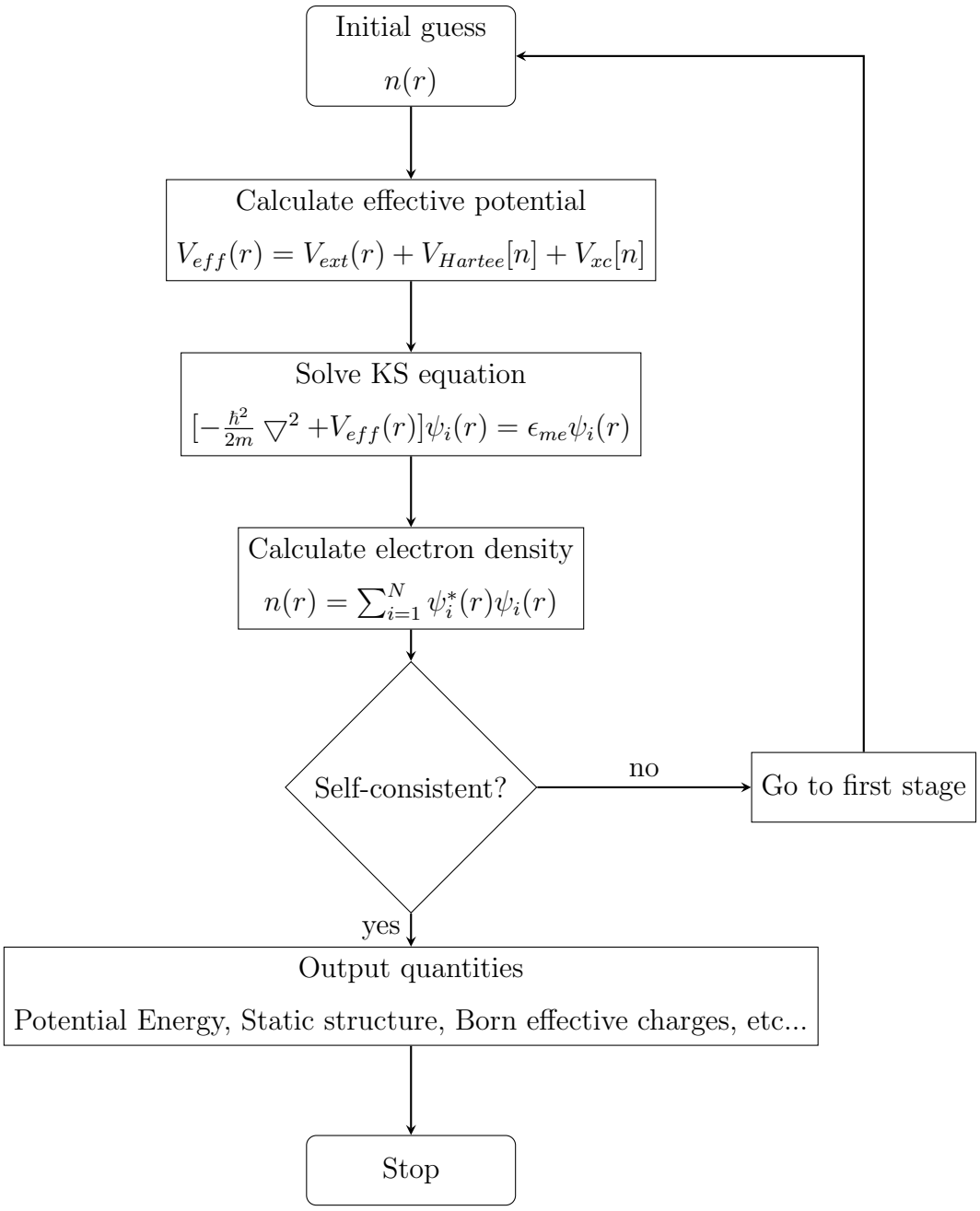

2.9 Exchange-correlation (XC) functionals

Jacob's Ladder of XC functionals Heaven of chemical accuracy. It is crucial to have an accurate XC energy functional $E_{XC}[n(\vec{r})]$ in order to give a satisfactory description of a realistic condensed matter system. The most widely used approximation for the XC potential are the local density approximation (LDA) and the generalized-gradient approximation (GGA).

2.9.1 Local (spin) Density Approximation (LDA)

The accuracy of DFT depends on its ability to approximate the unknown exchange-correlation (XC) part of the KS functional. The local density approximation (LDA) is the most common approximation to the XC potential V_{xc}. The LDA is traditionally based on knowledge of the energy of the infinite three-dimensional (3D) homogenous electron gas [20]. The XC energy per electron at a point $\vec{r}$ is considered the same as that for a homogeneous electron gas (HEG) that has the same electron density at the point $\vec{r}$. The total exchange-correlation functional $E_{XC}[n(\vec{r})]$ can be written as

$$\begin{aligned} E_{XC}^{LDA}[n(\vec{r})] &= \int n(\vec{r})\epsilon_{XC}^{hom}(n(\vec{r}))d\vec{r} \\ &= \int n(\vec{r})[\epsilon_{X}^{hom}(n(\vec{r})) + \epsilon_{C}^{hom}(n(\vec{r}))]d\vec{r} \\ &= E_{X}^{LDA}[n(\vec{r})] + E_{C}^{LDA}[n(\vec{r})] \end{aligned} \tag{2.72}$$

for spin unpolarized systems and

$$E_{XC}^{LSDA}[n_{\uparrow}(\vec{r}), n_{\downarrow}(\vec{r})] = \int n(\vec{r})\epsilon_{XC}^{hom}(n_{\uparrow}(\vec{r}), n_{\downarrow}(\vec{r}))d\vec{r} \tag{2.73}$$

for spin polarized systems [21], where the XC energy density $\epsilon_{XC}^{hom}(n(\vec{r}))$ is a function of the density alone, and is decomposed into exchange energy density $\epsilon_{X}^{hom}(n(\vec{r}))$ and correlation energy density $\epsilon_{C}^{hom}(n(\vec{r}))$ so that the XC energy functional is decomposed into exchange energy functional $E_{X}^{LDA}[n(\vec{r})]$ and correlation energy functional $E_{C}^{LDA}[n(\vec{r})]$ linearly. Note that $E_{XC}^{LSDA}[n_{\uparrow}(\vec{r}), n_{\downarrow}(\vec{r})]$ is not written in the way

$$E_{XC}^{LSDA}[n_{\uparrow}(\vec{r}), n_{\downarrow}(\vec{r})] = \int [n_{\uparrow}(\vec{r})\epsilon_{XC,\uparrow}^{hom}(n_{\uparrow}(\vec{r})) + n_{\downarrow}(\vec{r})\epsilon_{XC,\downarrow}^{hom}(n_{\downarrow}(\vec{r}))]d\vec{r} \tag{2.74}$$

as one may think. The exchange energy functional $E_{X}^{LDA}[n(\vec{r})]$ employs the expression for a HEG by using it point wise, which is known analytically as

$$E_{X}^{LDA}[n(\vec{r})] = \int n(\vec{r})\epsilon_{X}^{hom}(n(\vec{r}))d\vec{r} = -\frac{3}{4}(\frac{3}{\pi})^{\frac{1}{3}} \int n(\vec{r})^{\frac{4}{3}}d\vec{r} \tag{2.75}$$

where

$$\epsilon_X^{hom}(n(\vec{r})) = -\frac{3}{4}(\frac{3}{\pi})^{\frac{1}{3}} n(\vec{r})^{\frac{1}{3}} \tag{2.76}$$

is the exchange energy density of the unpolarized HEG introduced first by Dirac. Analytic expressions for the correlation energy of the HEG are unknown except in the high and low density limits corresponding to infinitely weak and infinitely strong correlations. The expression of the correlation energy density of the HEG at high density limit has the form

$$\epsilon_C = A\ln(r_s) + B + r_s(Cln(r_s) + D) \tag{2.77}$$

and the low density limit takes the form

$$\epsilon_C = \frac{1}{2}(\frac{g_0}{r_s} + \frac{g_1}{r_s^{\frac{3}{2}}} + ...) \tag{2.78}$$

where the Wigner-Seitz radius r_s is related to the density as

$$\frac{4}{3}\pi r_s^3 = \frac{1}{n}. \tag{2.79}$$

In order to obtain accurate values of the correlation energy density at intermediate density, accurate quantum Monte Carlo (QMC) simulations for the energy of the HEG are needed and have been performed at several intermediate density values. Most local density approximations to the correlation energy density interpolate these accurate values from QMC simulations while reproducing the exactly known limiting behaviour. Depending on the analytic forms used for ϵ_C, different local density approximation imations were proposed including Vosko-Wilk-Nusair [22] (VWM), Perdew-Zunger [23], Cole-Perdew [24] (CP) and Perdew-Wang [25] (PW92). For spin polarized systems, the exchange energy functional is known exactly from the result of spin-unpolarized functional:

$$E_X[n_\uparrow(\vec{r}), n_\downarrow(\vec{r})] = \frac{1}{2}(E_X[2n_\uparrow(\vec{r})] + E_X[2n_\downarrow(\vec{r})]) \tag{2.80}$$

The spin-dependence of the correlation energy density is approached by the relative spin-polarization:

$$\zeta(\vec{r}) = \frac{n_\uparrow(\vec{r}) - n_\downarrow(\vec{r})}{n_\uparrow(\vec{r}) + n_\downarrow(\vec{r})} \tag{2.81}$$

The spin correlation energy density $\epsilon_C(n(\vec{r}), \zeta(\vec{r}))$ is so constructed to interpolate extreme values $\zeta = 0, \pm 1$, corresponding to spin-unpolarized and ferromagnetic situations. The XC potential $V_{XC}(\vec{r})$ in LDA is

$$V_{XC}^{LDA} = \frac{\delta E_{XC}^{LDA}}{\delta n(\vec{r})} = \epsilon_{XC}(n(\vec{r})) + n(\vec{r})\frac{\partial \epsilon_{XC}(n(\vec{r}))}{\partial n(\vec{r})} \tag{2.82}$$

Within LDA, the total energy of a system is:

$$\begin{aligned}
E_{tot}[n(\vec{r})] &= T_S[n(\vec{r})] + E_H[n(\vec{r})] + E_{XC}[n(\vec{r})] + \int n(\vec{r}) V_{ext}(\vec{r}) d\vec{r} \\
&= \sum_i^{occ.} \langle \Psi_i(\vec{r})| -\frac{1}{2}\nabla^2 |\Psi_i(\vec{r})\rangle + E_H[n(\vec{r})] + E_{XC}[n(\vec{r})] + \int n(\vec{r}) V_{ext}(\vec{r}) d\vec{r} \\
&= \sum_i^{occ.} \langle \Psi_i(\vec{r})| -\frac{1}{2}\nabla^2 + V_H(\vec{r}) + V_{XC}(\vec{r}) + V_{ext}(\vec{r}) |\Psi_i(\vec{r})\rangle \\
&- \sum_i^{occ.} \langle \Psi_i(\vec{r})| V_H(\vec{r}) |\Psi_i(\vec{r})\rangle - \sum_i^{occ.} \langle \Psi_i(\vec{r})| V_{XC}(\vec{r}) |\Psi_i(\vec{r})\rangle \\
&- \sum_i^{occ.} \langle \Psi_i(\vec{r})| V_{ext}(\vec{r}) |\Psi_i(\vec{r})\rangle + E_H[n(\vec{r})] + E_{XC}[n(\vec{r})] + \int n(\vec{r}) V_{ext}(\vec{r}) d\vec{r} \\
&= \sum_i^{occ.} \varepsilon_i - \frac{1}{2}\int \frac{[n(\vec{r})][n(\vec{r}')]}{|\vec{r} - \vec{r}'|} d\vec{r} d\vec{r}' + \int n(\vec{r})(\epsilon_{XC}(\vec{r}) - V_{XC}(\vec{r})) d\vec{r} \\
&= \sum_i^{occ.} \varepsilon_i - \frac{1}{2}\int \frac{[n(\vec{r})][n(\vec{r}')]}{|\vec{r} - \vec{r}'|} d\vec{r} d\vec{r}' + \int n(\vec{r})^2 \frac{\partial \epsilon_{XC}(n(\vec{r}))}{\partial n(\vec{r})} d\vec{r}
\end{aligned} \tag{2.83}$$

As mentioned before, $E_{tot} \neq \sum_i^{occ.} \varepsilon_i$. The LDA is very simple, correlation to the exchange-correlation energy due to the inhomogeneities in the electronic density are ignored. However it is surprisingly successful and even works reasonably well in systems where the electron density is rapidly varying. One reason is that LDA gives the correct sum rule to the exchange-correlation hole. That is, there is a total electronic charge of one electron excluded from the neighborhood of the electron at $\vec{r}$. In the meantime, it tends to underestimate atomic ground state energises and ionization energies, while overestimating binding energies. It makes large errors

in predicting the energy gaps of some semiconductors. Its success and limitations lead to approximations of the XC energy functional beyond the LDA, through the addition of gradient corrections to incorporate longer range gradient effects (GGA), as well as LDA+U method to account for the strong correlations of the d electrons in transition elements and f electrons in lanthanides and actinides.

2.9.2 Generalized-Gradient Approximation (GGA)

As mentioned above, the LDA neglects the inhomogeneities of the real charge density which could be significantly different from the HEG result. This leads to the development of various generalized-gradient approximations (GGAs) which include density gradient corrections and higher spatial derivatives of the electron density and give better results than LDA in many cases. Three most widely used GGAs are the forms proposed by Becke (B88) [26], Perdew *et al*. [27], and Perdew, Burke and Enzerhof (PBE) [28]. The definition of the XC energy functional of GGA is the generalized form in Eq.(2.73) of LSDA to include corrections from density gradient $\nabla n(\vec{r})$ as

$$\begin{aligned} E_{XC}^{GGA}[n_\uparrow(\vec{r}), n_\downarrow(\vec{r})] &= \int n(\vec{r})\epsilon_{XC}^{hom}(n_\uparrow(\vec{r}), n_\downarrow(\vec{r}), |\nabla n_\uparrow(\vec{r})|, |\nabla n_\downarrow(\vec{r})|, ...)d\vec{r} \\ &= \int n(\vec{r})\epsilon_{XC}^{hom}(n_\uparrow(\vec{r}), n_\downarrow(\vec{r}), |\nabla n_\uparrow(\vec{r})|, |\nabla n_\downarrow(\vec{r})|, ...)d\vec{r} \end{aligned} \quad (2.84)$$

Where F_{xc} is dimensionless and $\epsilon_X^{hom}(n(\vec{r}))$ is the exchange energy density of the unpolarized HEG as given in Eq. (2.76). F_{xc} can be decomposed linearly into exchange contribution F_x and correlation contribution F_c as $F_{xc} = F_x + F_c$. GGA generally works better than LDA, in predicting bond length and binding energy of molecules, crystal lattice constants, and so on, especially in systems where the charge density is rapidly varying. However GGA sometimes overcorrects LDA result in ionic crystals where the lattice constants from LDA calculations fit well with experimental data but GGA will overestimate it. Nevertheless, both LDA and GGA perform badly in materials where the electrons tend to be localized and strongly correlated such as transition metal oxides and rare-earth elements and compounds. This drawback leads to approximations beyond LDA and GGA.

Chapter 3

Electronic, magnetic and optical properties of CeP

Cerium phosphide (CeP) is a cerium-phosphorus inorganic compound with the formula CeP. Phosphanylidynecerium is the IUPAC name for this chemical. Ce is a rare earth metal with strong acidic and oxidizing properties, whereas P is a highly reactive non-metallic element in the CeP combination. It is very unstable and does not dissolve in water. With a molecular weight of 171.09, it has a cubic crystalline structure.

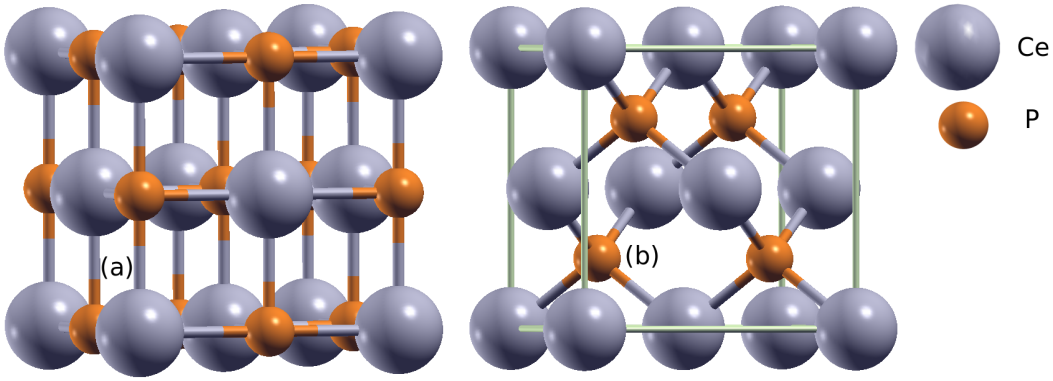

Figure 3.1: Crystal structure of CeP (a) rock salt and (b) zinc-blende type obtained with XCrySDen.

3.1 Method of calculations

Based on first principles calculation the self-consistent scheme are utilized to investigate the electronic, magnetic and optical characteristics of CeP structures. For this purpose we use here WIEN2k code, which can solve the Khon-Sham equations. We choose appropriate approximation for determining the exchange and correlation energy in Khon-Sham equation, which provides a significant impact on the accuracy of the final result. The RKmax, K-points, and lattice constant parameters are optimized by using the GGA and mBJ potential but band structure, DOS, and optical properties are calculated using only the mBJ potential. RKmax = 8.5 is the maximum mutual lattice vector utilized in plane wave dilation, and Rmt is the lowest radius of the muffin-tin sphere. After optimizing the energy, we set this value. The sizes of the muffin-tin spheres were chosen to be 2.3 a.u. for both Ce and P atoms. The largest possible vector in charge density Fourier expansion (Gmax) has a magnitude of twelve. Energy and charge convergence criterion are based on 0.00001 Ry and 0.0001 e, respectively. There was a cut-off energy of -6 Ry that separated the valence electrons from the core electrons. There are $10 \times 10 \times 10$ K-points in the Brillouin zone that we used for energy calculations, which is 1000 K-points in the total zone. Since denser mesh of K-points is required to calculate density of states and transport properties, therefore we used 5000 K-points in the entire Brillouin zone, or $17 \times 17 \times 17$ in the irreducible Brillouin zone.

3.2 Geometric structure and volume optimization

The stability of any compound in the structure must first be checked before the electronic or magnetic properties calculations. We run volume optimization calculation for both GGA and mBJ potential to obtain the best theoretical lattice parameters and minimum energy value [30] which are the closest to experimental value. We run this calculation for both ferromagnetic and non-magnetic phase [Figure 3.2]. The equilibrium energy of RS type structure is lower than that of ZB type, also the same thing happen for lattice constant parameter (Table 3.1). For this purpose we use the Murnaghan equation of state [31]. From the volume vs energy plotting

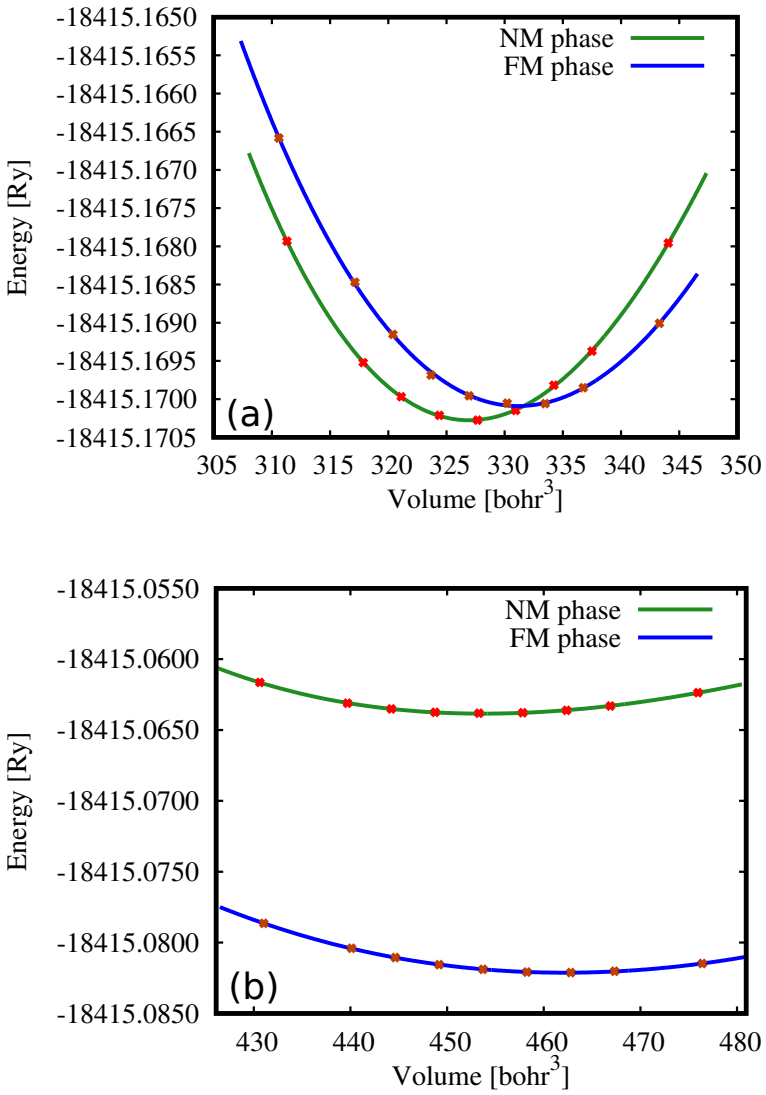

Figure 3.2: Volume optimization of CeP in (a) rock salt and (b) zinc-blende type structure.

we can get the most stable structure of CeP and based on this structure the future electronic and magnetic property is calculated. The unit cell of CeP shows in Figure 3.1 obtained by using XCrysDen software. The RMT value for both atom is 2.3 and space group of RS type structure is Fm-3m (#225) with Ce atom at (0,0,0) position and P atom at (0.5,0.5,0.5) position. In the ZB type structure the space group is F-43m (#216). Here the position of Ce atom occupies at the same (0,0,0) site, but the P atom located at (0.25,0.25,0.25) site. These value of space group and atomic position of CeP compound are taken from reference [32].

Table 3.1: Equilibrium energy and lattice constant of CeP in ferromagnetic and non-magnetic phases.

Compound	Structure type	Calculation	Lattice constant (Å)	Equilibrium energy (Ry)
CeP	RS	NM	5.79	-18415.17
		FM	5.41	-18415.17
	ZB	NM	6.45	-18415.06
		FM	6.49	-18415.08

3.3 Electronic properties

The density of state (DOS) and the electronic band structure are well-known parameters for determining the electronic properties. To compute the DOS and band structure, we used the mBJ potential for both spin polarized and non-spin polarized calculations.

3.3.1 Band structure

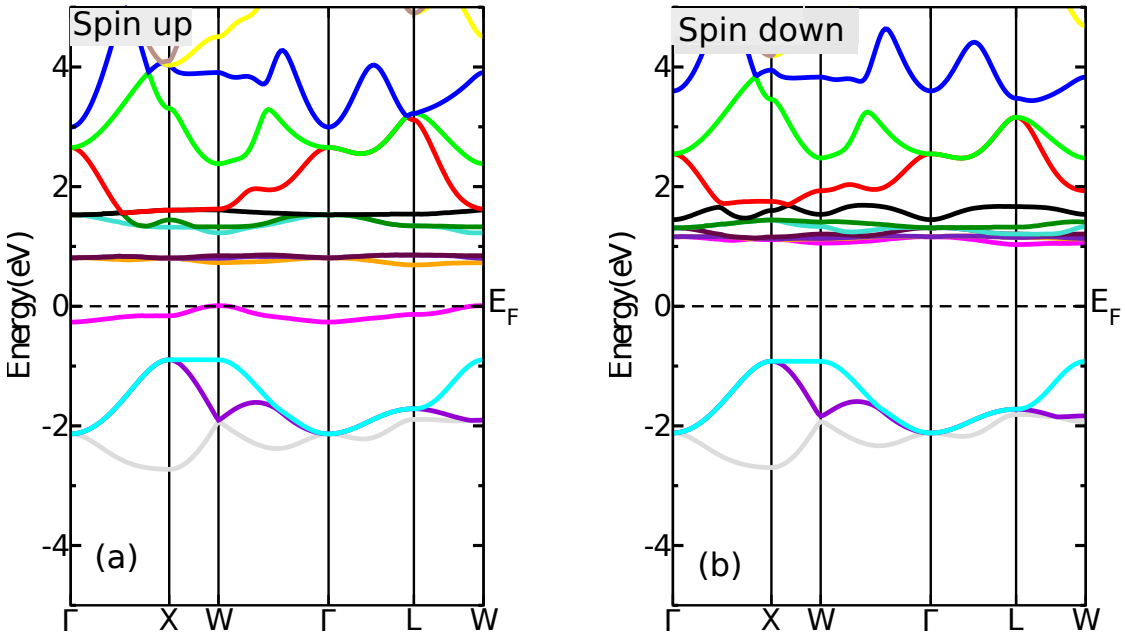

Figure 3.3: Band structure of CeP zinc-blende type structure in spin up (a) and down (b) channel.

In the field of electronic characteristics, the electronic band structure and density of

state (DOS) are well-known parameters that we calculate for our compound CeP. Figure 3.3 and Figure 3.4 illustrates the calculated spin up and down energy bands both for ZB and RS type structure respectively. While Figure 3.5 represent the non-magnetic calculation for both structure. The calculation is done by defining highly symmetric points on the edge of the Brillouin zone with sampling path of $\Gamma - X - W - \Gamma - L - W$. Since the energy values (E) are shown in relation to the Fermi energy (E_F), so the fermi level is represented by 0 eV.

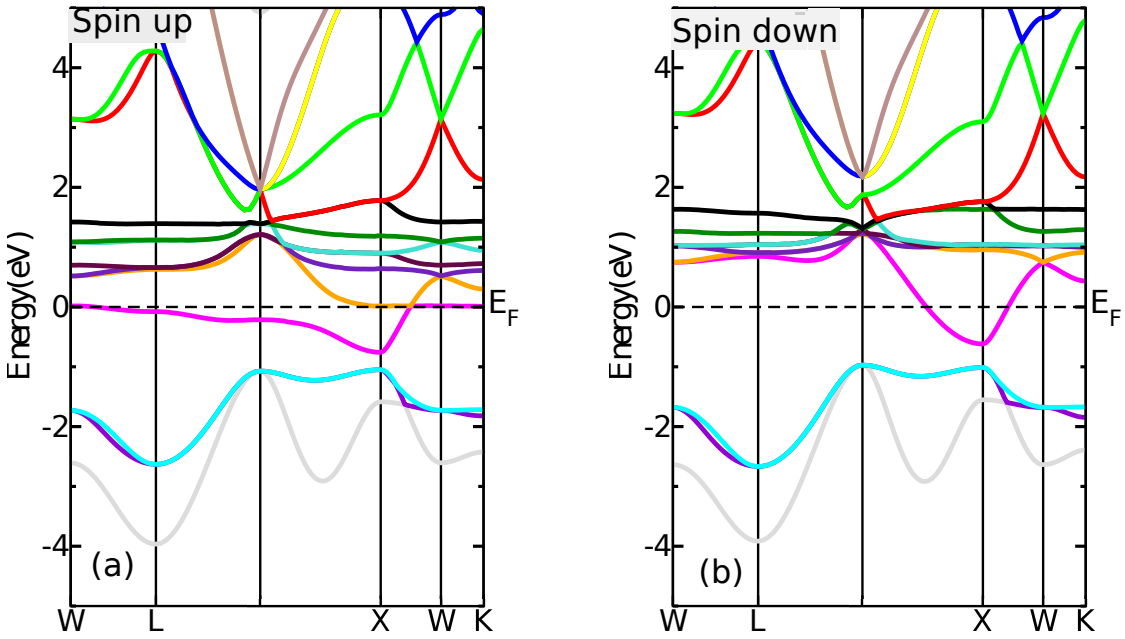

Figure 3.4: Band structure of CeP rock salt type structure in spin up (a) and down (b) channel.

The conduction and valence band intersect at Fermi level are shown in Figure 3.4(a,b) and 3.5(b) indicating CeP has metallic characteristics for RS type structure, also the same things happen for non-spin ZB type structure [Figure 3.5(a)]. While the band gap for both spin up and down bands can be readily seen in Figure 3.3(a,b) which indicates the semiconducting behavior of CeP for ZB type structure. The lowest valence band in the up spin channel is for p band of the P atom, which has an energy of -2.2 eV at the Γ point. The highest valence band at W point is the f band of the Ce atom, which is in contact with Fermi level E_F. Above the Fermi

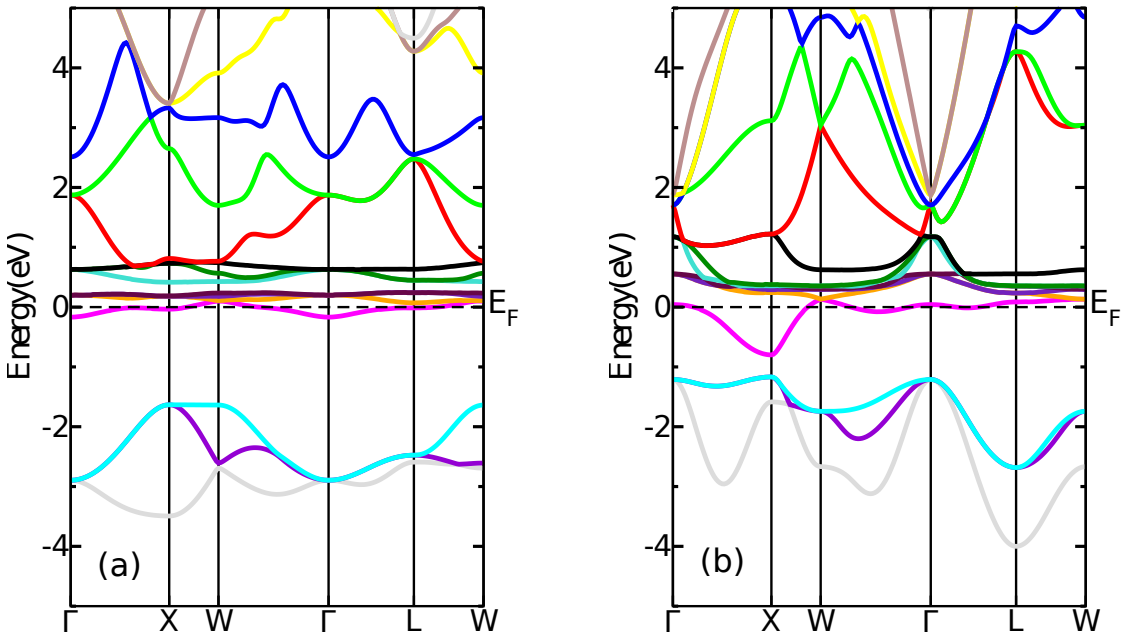

Figure 3.5: Band structure of CeP (a) zinc-blende and (b) rock salt type structure for non-magnetic calculation.

energy level E_F, the lowest conduction band is the f band at the L point, which creates an indirect band gap of 0.689 eV between a maximum valence band at the W point and a minimum conduction band at the L point. Also in case of down spin channel maximum valence band occurs at the W point but minimum conduction band at the L point which provides the comparable larger value of indirect gap of 1.951 eV. The calculated energy band gap (in eV) of CeP in both GGA and mBJ approaches is tabulated in Table 3.2.

3.3.2 Density of state

The number of states for each period of energy which are occupied by the specific energy levels is usually explained by the density of states (DOS) of the system. The total and partial DOS are calculated within the magnetic phase designed for spin up and down channel are also measured by utilizing the mBJ potential to find electronic characteristics of CeP clearly, as shown in Figure 3.6 and Figure 3.7. The total number of states per unit energy range (in eV) is plotted on the Y-axis, and the corresponding energy (in eV) is plotted on the X-axis, both with reference to

the Fermi energy. The Fermi energy was set to 0 eV in this case. We can see that there is a band gap between the valence and conduction bands for both up and down channel in ZB type structure. This value is 0.7 eV for up spin and 2.0 eV for down spin. Which gives ZB type structure of CeP shows the semiconducting behaviour for it ferromagnetic calculation. The orbital contribution of this satructure shows that f state of Ce atom gives an majority contribution in the conduction band of both up and down spin channel. For down spin channel a strong peak is obtain at 1.6 eV energy value. Whereas in the up spin channel we get three small peak between 1.4 eV to 2 eV energy value. In comparison with f state, d state gives negligible contribution in both valence and conduction band. The orbital contribution of P atom shows that the p states gives a very small contribution in the energy range from -0.4 eV to -2.7 eV. Whereas the d state of this atom gives negligible contribution. The RS type structure of CeP shows that there is no gap between conduction and valence band, indicating the metallic behavior of this structure. The orbital contribution for this structure shows almost same behavior as ZB type structure. Here f state of Ce atom gives the majority contribution in the conduction band. In the valence band p state of P atom gives very small contribution from -1.6 eV to -4 eV energy range.

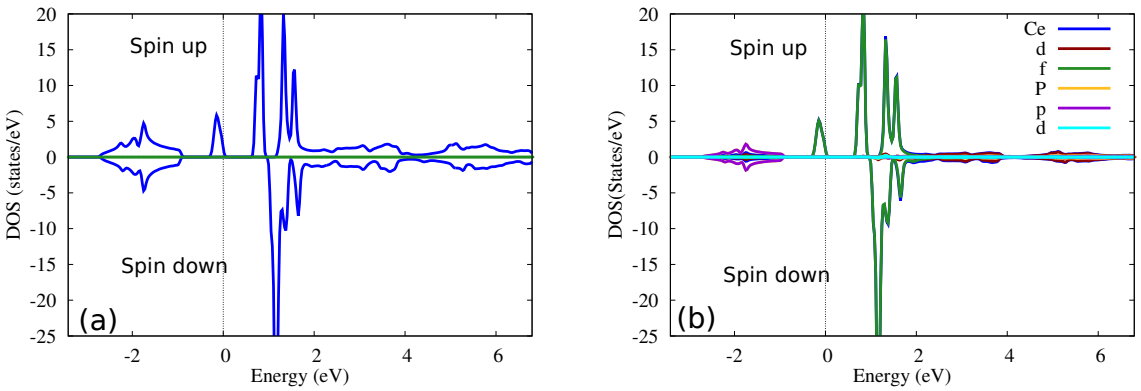

Figure 3.6: The spin-polarized total densities of states (DOS) and partial DOSs of CeP in zinc-blende type structure calculated at equilibrium lattice constant.

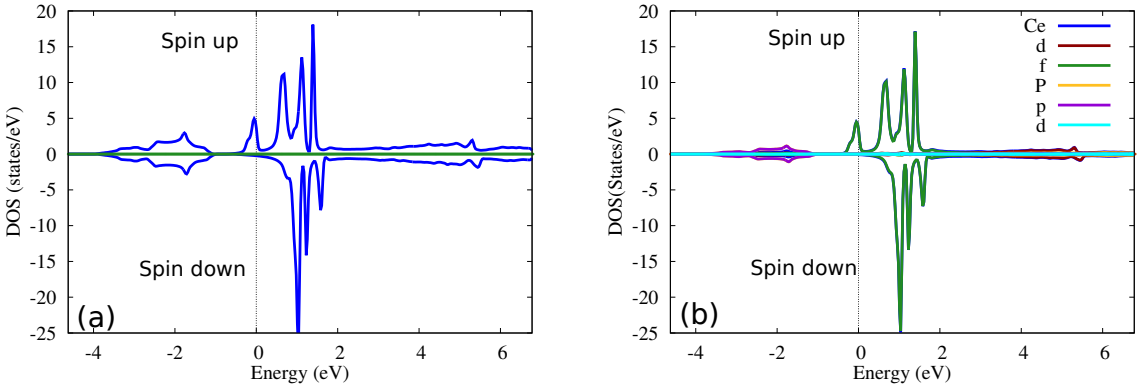

Figure 3.7: The spin-polarized total densities of states (DOS) and partial DOSs of CeP in rock salt type structure calculated at equilibrium lattice constant.

Table 3.2: Energy band gap (in eV) of CeP with GGA and mBJ approaches.

Compound	Structure type	Method	Band gap (eV)	
			Spin up	Spin down
CeP	ZB	GGA	0.078	1.663
		mBJ	0.689	1.951

3.4 Magnetic properties

The ferromagnetic ordering in CeP is revealed by the spin-polarized calculation. Furthermore, estimated magnetic moments of individual atoms (Table 3.3) helps to understood the electronic property results. Ce atoms are responsible for the majority of the total magnetic moment. For both mBJ and GGA potential, the ZB type structure of CeP compound has an integer-value total magnetic moment of 1.00 μ_B, which follows the Slater-pauling rule of $M_t = Z_t - 8$ [33]. In case of RS type structure we get a non-integer value of 0.67 μ_B for GGA potential and 0.88 μ_B for mBJ potential. The partial magnetic moments of Ce and P are antiparallel, indicating that CeP carry ferromagnetic characteristics.

3.5 Optical property

Optical properties help us to understood the nature of materials and provide us a clear image of how we might use them in optoelectronic devices. Within the mBJ approximation, dielectric function, optical reflectivity, conductively, refractive index,

Table 3.3: Total spin magnetic moment of CeP in GGA and mBJ approaches.

Compound	Structure type	Individual magnetic moment (μ_B)		
		Site	GGA	mBJ
CeP	ZB	Intersititial	0.15	0.1
		Ce	0.88	0.91
		P	-0.03	-0.02
		Total	1	1
	RS	Intersititial	0.14	0.09
		Ce	0.56	0.79
		P	-0.03	-0.01
		Total	0.66	0.88

absorption coefficient, and electron energy loss of CeP are determined. Calculation of the complex dielectric function as illustrated in Figure 3.8 is one of the best techniques to investigating the optical properties of materials [34]. Which can be represented as, $\varepsilon(\omega) = \varepsilon_1(\omega) + i\varepsilon_2(\omega)$, where $\varepsilon_1(\omega)$ and $\varepsilon_2(\omega)$ are the real and imaginary components of dielectric function respectively. There is no transition of RS type structure and non-magnetic phase of ZB type structure because it has a negative value and the incident electromagnetic waves are totally reflected. In case of magnetic phase the ZB type structure shows positive value, indicating that it is related to the EM wave propagation. The static values of $\varepsilon_1(0)$ in the ZB type magnetic phase is 25.5 and also when the energy is increases, the value of real dielectric function $\varepsilon_1(\omega)$ approaches to zero. The maximum value of RS type FM phase, RS type NM phase, ZB type FM phase and ZB type NM phase were 10.3, 15.3, 10.6 and 10.2 respectively. The energy absorption by the materials is represented by the imaginary part of the dielectric function $\varepsilon_2(\omega)$, which is also linked to the energy band structure. Strong optical transitions are caused by the greatest peak of the imaginary component of the dielectric constant, which is positioned between 0 and 0.5 eV energy range for both structures.

Reflectivity is utilized to determine whether a substance may be employed as an anti-reflecting coating for shielding purpose, shown in Figure 3.9(a). According to the EM spectrum the energy of the IR ray is 0.12 eV, in this area of energy we have

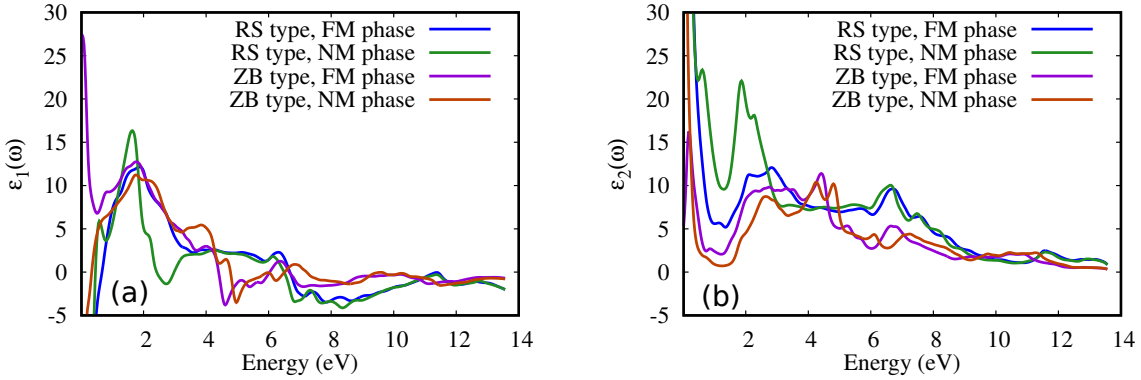

Figure 3.8: Calculated (a) Real $\varepsilon_1(\omega)$ and (b) Imaginary $\varepsilon_2(\omega)$ part of dielectric function of CeP as a function of energy.

a high value of reflectivity. The visible region spans the energy range of 1.8 eV to 3.1 eV and there is no highest peak value in this range, has a medium reflectivity value. In the vacuum UV zone, the reflectivity increases and reaches to it maximum value. For the ZB type structure, the greatest peak is 12 eV, while for the RS type structure, it is 8.8 eV. As a result, in the high-energy vacuum UV region, CeP is a good reflector. The ability of a medium to generate a conduction phenomenon as electromagnetic radiation attempts to propagate through it is determined by optical conductivity. In Figure 3.9(b), we can see the optical conductivity graph. It is observe that as energy increases, the conductivity increases as well. For the RS type NM phase, the greatest conductivity peak is found in the 6.5 eV energy range. Optical conductivity begins to decrease at 6.5 eV and eventually disappears for higher energy values. Which suggests that CeP could be a good material for optoelectronics. The refractive index of CeP as shown in Figure 3.9(c), is another important physical quantity that describes the optical properties of that compound. The refractive index of material is increases with decreasing the speed of light as it travels from one medium to another. The refractive indices are also known to be inversely related to the band gap, with the band gap decreasing as the refractive index rises. The largest refractive index value is found in the infrared region and decreases with increasing energy at the visible and other region, as shown in this graph. It is the most basic optical parameter for calculating how much energy a material absorbs. We can see in Figure 3.9(d), the absorption coefficient has no sharp peak in the IR and visible energy ranges, implies that CeP can conduct both visible and IR rays. The highest value of absorption peaks are obtained with higher

energies. All of this behavior can help the materials optoelectronic qualities. As shown in Figure 3.9(e), the electron energy loss is an important factor in describing the energy loss of a fast moving electron in a material. It is common knowledge that the main peak in electron energy loss spectra exhibits the characteristic associated with plasma resonance and its frequency ω_p. The opaqueness of the compounds is evidenced by the high peak in electron energy loss just after 4 eV.

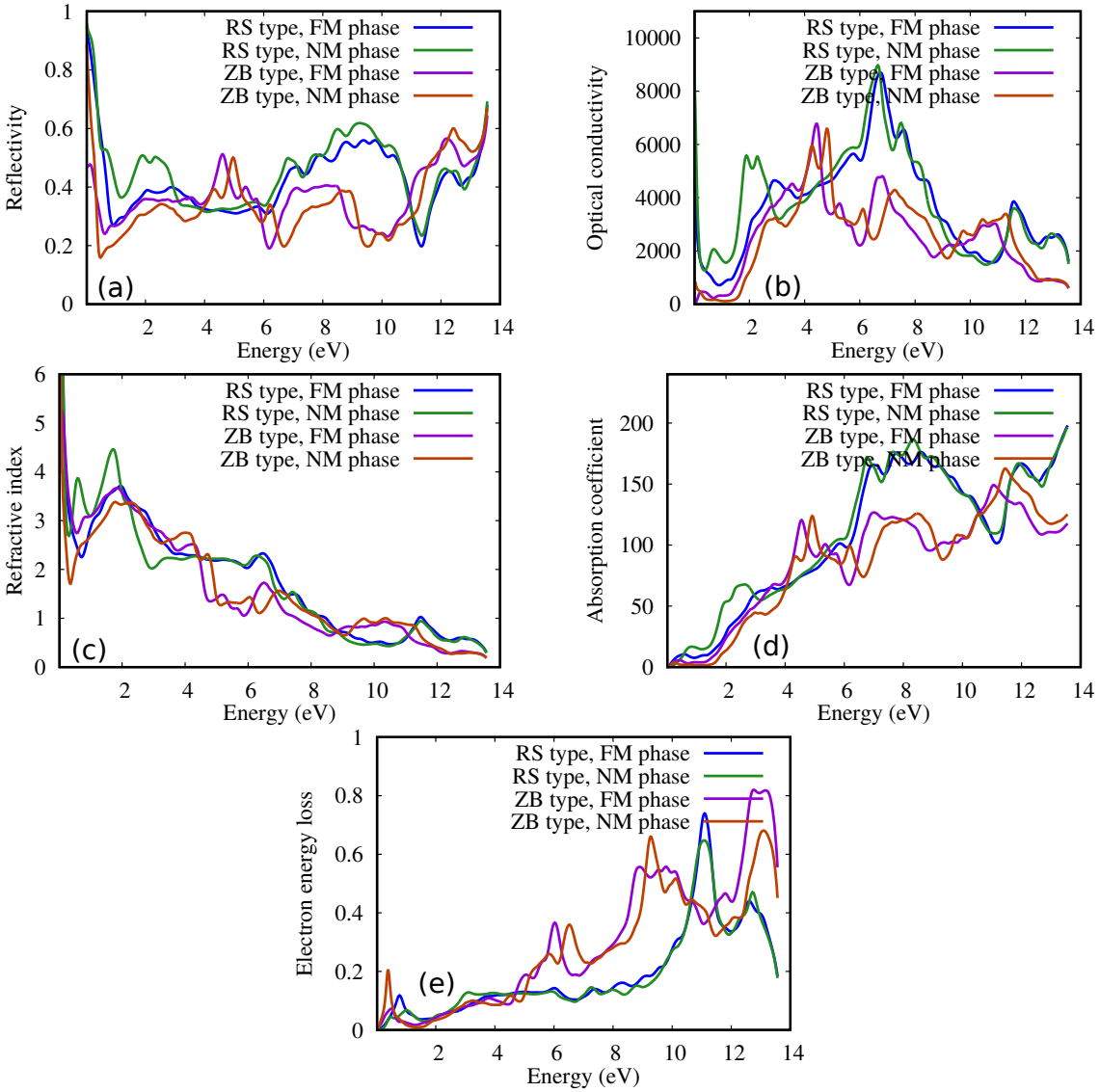

Figure 3.9: Calculated optical (a) reflectivity, (b) conductivity, (c) refractive index, (d) absorption coefficient, and (e) electron energy loss of CeP as a function of energy.

Chapter 4

Conclusions

We used first-principle calculations to investigate the electronic, magnetic, and optical properties of CeP, a rare-earth phosphide. The intriguing property of CeP being more stable in the ferromagnetic phase for both ZB and RS type structures with lattice parameters 5.41 and 6.49 Å respectively is obtained via volume optimization. We find an indirect band gap of 0.689 and 1.951 eV in spin up and down channel respectively for ZB type magnetic phase within mBJ potentials. The electronic band structure and DOS calculations reveal the semiconducting behavior of CeP for it ZB type structure. This type structure has an integer-valued total magnetic moment of μ_B, corresponding to the Slater-Pauling rule, where Ce atom gives the majority contribution. In case of optical property the optical reflectivity, conductivity, refractive index, absorption coefficient, and electron energy loss at photon energies up to 14.0 eV is used to investigate the optical nature of CeP. Our computed electronic, magnetic, and optical properties demonstrate that CeP is a good choice for optoelectronic applications.

List of Abbreviations

BZ	:	Brillouin Zone
DFT	:	Density Functional Theory
DOS	:	Density of States
XC	:	Exchange correlation
FM	:	Ferromagnetic
FP-LAPW	:	Full potential linearized augmented plane waves
GGA	:	Generalized Gradient Approximation
HK	:	Hohenberg-Kohn
HEG	:	Homogeneous electron gas
KS	:	Kohn-Sham
LSDA	:	Local Spin Density Approximation
NM	:	Non-magnetic
RS	:	Rock salt
ZB	:	Zinc-blende

Bibliography

[1] Daniel Steigerwald, Serge Rudaz, Heng Liu, R Scott Kern, Werner Götz, and Robert Fletcher. Iii–v nitride semiconductors for high-performance blue and green light-emitting devices. *Jom*, 49(9):18–23, 1997.

[2] PJ McCann. Iv–vi semiconductors for mid-infrared optoelectronic devices. In *Mid-infrared Semiconductor Optoelectronics*, pages 237–264. Springer, 2006.

[3] G Busch. Magnetic properties of rare-earth compounds. *Journal of Applied Physics*, 38(3):1386–1394, 1967.

[4] GY Gao, KL Yao, ZL Liu, J Zhang, Y Min, and SW Fan. A first-principles study of half-metallic ferromagnetism in binary alkaline-earth nitrides with rock-salt structure. *Physics letters A*, 372(9):1512–1515, 2008.

[5] GY Gao, KL Yao, MH Song, and ZL Liu. Half-metallic ferromagnetism in rocksalt and zinc-blende ms (m= li, na and k): a first-principles study. *Journal of magnetism and magnetic materials*, 323(21):2652–2657, 2011.

[6] O Krogh Andersen. Linear methods in band theory. In *The Electronic Structure of Complex Systems*, pages 11–66. Springer, 1984.

[7] P Blaha. Wien2k, an augmented plane wave local orbitals program for calculating crystal properties karlheinz schwarz. *Techn. Universität Wien, Austria*, 2001.

[8] Pierre Hohenberg and Walter Kohn. Inhomogeneous electron gas. *Physical review*, 136(3B):B864, 1964.

[9] Niklas Zwettler. Density functional theory.

[10] Wolfram Koch and Max C Holthausen. *A chemist's guide to density functional theory*. John Wiley & Sons, 2015.

[11] Nouredine Zettili. Quantum mechanics: concepts and applications, 2003.

[12] Klaus Capelle. A bird's-eye view of density-functional theory. *Brazilian journal of physics*, 36:1318–1343, 2006.

[13] Max Born and J Robert Oppenheimer. On the quantum theory of molecules. 1927.

[14] Paul Adrien Maurice Dirac. A new notation for quantum mechanics. In *Mathematical Proceedings of the Cambridge Philosophical Society*, volume 35, pages 416–418. Cambridge University Press, 1939.

[15] Christian B Lang and Norbert Pucker. *Mathematische methoden in der physik*, volume 2. Springer, 2005.

[16] Per-Olov Löwdin. Scaling problem, virial theorem, and connected relations in quantum mechanics. *Journal of Molecular Spectroscopy*, 3(1-6):46–66, 1959.

[17] E Fermi. Rend. accad. naz. lincei. 1927.

[18] Dennis P Clougherty and Xiang Zhu. Stability and tellers theorem: Fullerenes in the march model. *Physical Review A*, 56(1):632, 1997.

[19] Haozhao LIANG. Fundamentals of density functional theory & selected progress in ab initio nuclear dft. 2017.

[20] C-O Almbladh, U Von Barth, and R Van Leeuwen. Variational total energies from ϕ-and ψ-derivable theories. *International Journal of Modern Physics B*, 13(05n06):535–541, 1999.

[21] Ulf Von Barth and Lars Hedin. A local exchange-correlation potential for the spin polarized case. i. *Journal of Physics C: Solid State Physics*, 5(13):1629, 1972.

[22] SH Vosko, L Wilk, and M Nusair. Can. j. phys. 1980.

[23] John P Perdew. Density-functional approximation for the correlation energy of the inhomogeneous electron gas. *Physical Review B*, 33(12):8822, 1986.

[24] LA Cole and JP Perdew. Self-interaction correction to density-functional approximations for many-electron systems. *Phys. Rev. A: At., Mol., Opt. Phys*, 25:1265, 1982.

[25] John P Perdew. Jp perdew and y. wang, phys. rev. b 45, 13244 (1992). *Phys. Rev. B*, 45(13244):60, 1992.

[26] Axel D Becke. Density-functional exchange-energy approximation with correct asymptotic behavior. *Physical review A*, 38(6):3098, 1988.

[27] John P Perdew, John A Chevary, Sy H Vosko, Koblar A Jackson, Mark R Pederson, Dig J Singh, and Carlos Fiolhais. Atoms, molecules, solids, and surfaces: Applications of the generalized gradient approximation for exchange and correlation. *Physical review B*, 46(11):6671, 1992.

[28] John P Perdew, Kieron Burke, and Matthias Ernzerhof. Generalized gradient approximation made simple. *Physical review letters*, 77(18):3865, 1996.

[29] B Bhattarai, T Dahal, and NP Adhikari. First principles study of thermoelectric properties of skutterudites: Ir4sb12 and ca0. 04ir4sb12. *Journal of Nepal Physical Society*, 6(2):1–9, 2020.

[30] Murat Aycibin and ECE Naciye. First-principles calculation of the electronic and optical properties of birho 3 compound. *AIMS Materials Science*, 4(4):894–904, 2017.

[31] FD Murnaghan. The compressibility of media under extreme pressures. *Proceedings of the national academy of sciences of the United States of America*, 30(9):244, 1944.

[32] Ikram Un Nabi Lone, M Sirajuddeen, Saubia Khalid, and Hafiz Hamid Raza. First-principles study on electronic, magnetic, optical, mechanical, and thermodynamic properties of semiconducting gadolinium phosphide in gga, gga+ u, mbj, gga+ soc and gga+ soc+ u approaches. *Journal of Superconductivity and Novel Magnetism*, 34(5):1523–1538, 2021.

[33] Iosif Galanakis and Phivos Mavropoulos. Zinc-blende compounds of transition elements with n, p, as, sb, s, se, and te as half-metallic systems. *Physical Review B*, 67(10):104417, 2003.

[34] GK BALCI and S AYHAN. The first principle study: structural, electronic and optical properties of x2znn2 (x: Ca, ba, sr). *Journal of Non-Oxide Glasses Vol*, 11(1):9–18, 2019.